Applied Physics Letters

Direct synthesis of biaxially textured nickel disilicide thin films by magnetron sputter deposition on low-cost metal tapes for flexible silicon devices

Cite as: Appl. Phys. Lett. **114**, 083502 (2019); https://doi.org/10.1063/1.5080283
Submitted: 07 November 2018 . Accepted: 13 February 2019 . Published Online: 28 February 2019

Yongkuan Li, Ying Gao, Yao Yao, Sicong Sun, Devendra Khatiwada, Sara Pouladi, Eduard Galstyan, Monika Rathi, Pavel Dutta, Alexander P. Litvinchuk, Jae-Hyun Ryou, and Venkat Selvamanickam

Applied Physics Letters ARTICLE scitation.org/journal/apl

Direct synthesis of biaxially textured nickel disilicide thin films by magnetron sputter deposition on low-cost metal tapes for flexible silicon devices

Cite as: Appl. Phys. Lett. **114**, 083502 (2019); doi: 10.1063/1.5080283
Submitted: 7 November 2018 · Accepted: 13 February 2019 ·
Published Online: 28 February 2019

Yongkuan Li,[1,2,3,a] Ying Gao,[1,2,3] Yao Yao,[1,2,3] Sicong Sun,[1,2,3] Devendra Khatiwada,[1,2,3] Sara Pouladi,[1,3] Eduard Galstyan,[1,2,3] Monika Rathi,[1,2,3] Pavel Dutta,[1,2,3] Alexander P. Litvinchuk,[3] Jae-Hyun Ryou,[1,2,3] and Venkat Selvamanickam[1,2,3]

AFFILIATIONS

[1]Department of Mechanical Engineering, University of Houston, Houston, Texas 77204, USA
[2]Advanced Manufacturing Institute, University of Houston, Houston, Texas 77204, USA
[3]Texas Center for Superconductivity, University of Houston, Houston, Texas 77204, USA

[a)]Author to whom correspondence should be addressed: yli78@uh.edu

ABSTRACT

Nickel silicides are widely used as contact materials for electronic devices based on silicon (Si). However, they have been predominantly fabricated by annealing separate Ni and Si phases which leads to phase and structural complexity. In this letter, direct epitaxial growth of a single-phase nickel disilicide ($NiSi_2$) thin film by sputter deposition of $NiSi_2$ is achieved on low-cost and flexible Hastelloy tapes which offers a promising route to fabricate low-cost, flexible electronic devices. Biaxially textured titanium nitride (TiN) is applied as the seeding layer and the diffusion barrier under $NiSi_2$. An epitaxial relationship of $(001)\langle 100\rangle NiSi_2 \parallel (001)\langle 110\rangle TiN$ is observed with an extra-large lattice mismatch (~10.3%) between $NiSi_2$ and TiN. Both the bonding similarity and the passivation effect by hydrogen promote the epitaxial growth of $NiSi_2$ on TiN. The flat and smooth $NiSi_2$ thin film consists of grains with a size of 50–100 nm. An epitaxially grown Si film on $NiSi_2$ further demonstrates the potential of manufacturing high-performance Si flexible electronics with $NiSi_2$/TiN/Hastelloy as the direct contact through this approach.

Nickel silicides have been widely studied due to their low resistivity and thermodynamic stability as contact materials for silicon (Si) electronic devices, with nickel monosilicide (NiSi) mostly applied in complementary metal–oxide–semiconductor (CMOS) devices[1] and nickel disilicide ($NiSi_2$) mostly applied in metal-oxide-semiconductor field-effect transistors (MOSFETs).[2] Compared to NiSi, $NiSi_2$ ultrathin layers have lower contact resistivity and Schottky barrier height on both strained and unstrained Si.[3] Furthermore, epitaxial $NiSi_2$ has lower resistivity and higher reliability than polycrystalline $NiSi_2$ as contacts to Si devices.[3] However, both single-crystalline NiSi and $NiSi_2$ are predominantly fabricated by annealing nickel (Ni) layers deposited onto Si wafers[2,4] or Ni clusters implanted into Si wafers.[5] Relying on the solid-phase-epitaxy process, epitaxial growth of $NiSi_2$ films is challenging due to the formation of intermediate phases including nickel silicide (Ni_2Si) and NiSi phases[6,7] and different interfacial structures.[8] Direct synthesis of epitaxial $NiSi_2$ thin films by magnetron sputter deposition of $NiSi_2$ is reported in this letter.

Further, rather than rigid silicon wafers, low-cost and flexible Hastelloy tapes (~50 μm) are used as the substrates for growth of epitaxial $NiSi_2$, with a buffer layer of ion-beam-assisted-deposition (IBAD) titanium nitride (TiN).[9,10] Flexible electronics made of inorganic materials have been extensively pursued in the past few decades.[11] However, nickel silicides are rarely synthesized and applied as the contact materials to flexible devices. Polycrystalline NiSi were fabricated on polyimide substrates and suffered from diffusion of carbon from the substrates.[12] In our approach, inorganic flexible materials[13–16] and devices[17,18] have been fabricated on the low-cost, flexible Hastelloy tapes which enables large-volume production by reel-to-reel processes. Compared to the previous works,[15,17] a significantly simplified buffer structure is used in this work, and the buffers of $NiSi_2$/TiN

simultaneously act as the bottom contacts to the devices. The buffer layer of TiN serves as both a seeding layer for epitaxial growth of single-crystalline $NiSi_2$ thin films and a diffusion barrier of impurities from the Hastelloy tapes owing to the excellent diffusion barrier property of TiN for various elements.[19–22] Growth of epitaxial Si films on $NiSi_2$ films demonstrates the great potential of our approach to fabricate low-cost, high-performance flexible electronics.

High-quality IBAD TiN templates were fabricated on Hastelloy C-276 substrates.[9] IBAD MgO templates based on Hastelloy C-276 substrates were used as referential substrates.[23] The IBAD TiN and MgO substrates included homo-epitaxial TiN and MgO films with thicknesses of ~150 nm and ~70 nm, respectively. The substrates were ultrasonically cleaned in an isopropyl alcohol (IPA) bath and then blown dry with nitrogen (N_2). A co-sputter deposition system with four targets and four magnetron sources was used. The chamber was pumped down to a base pressure of 2×10^{-7} Torr, and high-purity Ar (99.999%) and forming gas (Ar mixed with 4 vol. % H_2, 99.999%) were used for growth at a pressure of 4.20 mTorr. The target-substrate distance was set to 10 cm, and uniform growth was achieved by rotating the substrate holder at 20 rpm. For growth of all $NiSi_2$ films, a $NiSi_2$ target with a purity of 99.9% was used. The sputtering power, substrate temperature, and growth time were set to 300 W, 550 °C, and 30 min, respectively. The substrates and gases used for different samples discussed in this letter are listed in Table I. Growth parameters of a Si film on the $NiSi_2$ film of sample *c* are presented in supplementary material Part 1. A quartz crystal thickness monitor is used to achieve the same $NiSi_2$ film thickness among samples *a*, *b*, and *c*.

A triple-axis high-resolution X-ray diffractometer (HRXRD) (Rigaku Smartlab system) was used to collect θ-2θ scans and Rocking curves from the samples, and a Bruker 2D General Area Detector Diffraction System (GADDS) was used to obtain the X-ray pole figures. A LEO 1525 Scanning Electron Microscope (SEM) was employed to study the surface morphology. Transmission electron microscopy (TEM) was done with a JEOL 2000FX.

Epitaxial growth of $NiSi_2$ is found to be dependent on the type of templates and gases used, as studied with samples *a*, *b*, and *c*. The biaxial texture of the templates is demonstrated in Fig. 1, with TiN (002) and MgO (002) peaks in HRXRD θ-2θ scans as the unique orientations and fourfold symmetry detected in pole figures of both TiN and MgO. The $NiSi_2$ film of sample *a* exhibits $NiSi_2$ (111) and (220) peaks in θ-2θ scans as shown in Fig. 1(a), indicating that the film is not textured in out-of-plane. In contrast, when the IBAD MgO template is replaced by the IBAD TiN template, the $NiSi_2$ film of sample *b* shows a strong $NiSi_2$ (004) peak. Yet sample *b* is not totally textured, since a weak $NiSi_2$ (220) peak is also present. When an Ar-H_2 mixture is used in the growth of sample *c*, the $NiSi_2$ film shows a $NiSi_2$ (004) as the unique orientation, indicating that direct epitaxial growth of $NiSi_2$ is

TABLE I. Growth parameters of $NiSi_2$ thin films.

Sample	Template	Gas and flow (sccm)
a	IBAD MgO	Ar, 38
b	IBAD TiN	Ar, 38
c	IBAD TiN	Ar + H_2, 34.5

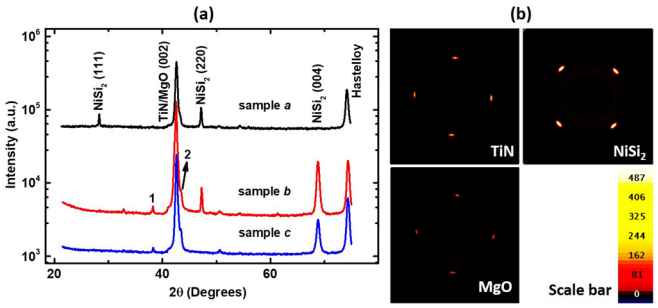

FIG. 1. (a) HRXRD θ-2θ scans of the $NiSi_2$ films of samples *a*, *b*, and *c*. Sample *a* is $NiSi_2$ grown on the IBAD MgO template using Ar, sample *b* is $NiSi_2$ grown on the IBAD TiN template using Ar, and sample *c* is $NiSi_2$ grown on the IBAD TiN template using Ar mixed with H_2. Peak 1 is a negligible TiN (111) peak (only shown on a log scale), and peak 2 is a Hastelloy peak. (b) {220} Pole figures of TiN and $NiSi_2$ of sample *c* and of MgO of the IBAD MgO template.

achieved by sputter deposition of $NiSi_2$ on the textured flexible substrate. This conclusion is confirmed by the fourfold symmetry of the $NiSi_2$ {220} pole figure shown in Fig. 1(b). Furthermore, the $NiSi_2$ is found to be free from twins, and the peak positions of $NiSi_2$ along ϕ are shifted by ~45° compared to those of TiN shown in Fig. 1(b), indicating an in-plane rotation between the two crystal lattices.

The different crystal structures of $NiSi_2$ in samples *a*, *b*, and *c* are further reflected in the SEM images in Fig. 2. The $NiSi_2$ thin film of sample *a* consists of grains with irregular shapes which corresponds to $NiSi_2$ oriented along (111) and (220) in Fig. 1(a). In sample *b*, when a strong $NiSi_2$ (004) peak appears, the grains become rounded. Some irregular grains still exist, which are most probably oriented along $NiSi_2$ (220). However, when an Ar-H_2 mixture is used as the process gas, a smooth and uniform surface morphology is observed in sample *c* which has a single out-of-plane orientation. The size of $NiSi_2$ grains is estimated to be 50–100 nm. The Hall measurement using an Ecopia HMS5000 system indicates metal-scale resistivities of the TiN and $NiSi_2$ thin films (supplementary material Part 2).

Direct epitaxial growth of $NiSi_2$ on flexible metal substrates is also observed in TEM analysis. Figure 3 displays the TEM image of sample *c* with a Si film further grown on $NiSi_2$. A uniform columnar structure is found in both TiN and $NiSi_2$ in Fig. 3(a); single-crystalline and twin-free patterns are observed in the selected area electron diffraction (SAED) shown in Fig. 3(c), which confirm the epitaxial growth of $NiSi_2$ on the IBAD TiN template. Further, the reciprocal lattices are marked as dashed lines in Fig. 3(c), which indicate that the zone axes are [100] for TiN and $[2\bar{2}0]$ for $NiSi_2$, confirming the ~45° in-plane rotation between them. The epitaxial relationship is then derived as $(001)\langle 100\rangle NiSi_2 \parallel (001)\langle 110\rangle TiN$. Figure 3(b) shows a SAED pattern at the Si-$NiSi_2$ interface and reveals a single-crystalline pattern for Si, which demonstrates the epitaxial growth of Si on $NiSi_2$ (XRD and SEM data of the Si film are reported in supplementary material Part 3). Compared to the Si films fabricated on Hastelloy tapes with buffers of germanium/cerium oxide/lanthanum manganate/magnesium oxide/yttrium oxide/aluminium oxide,[17] the buffers of $NiSi_2$/TiN applied in this paper are much more simplified and can simultaneously act as the bottom contact. Twins are observed in Si in Fig. 3(a) and are indicated by the twin spots in Fig. 3(b); such twins need to be eliminated by further studies.

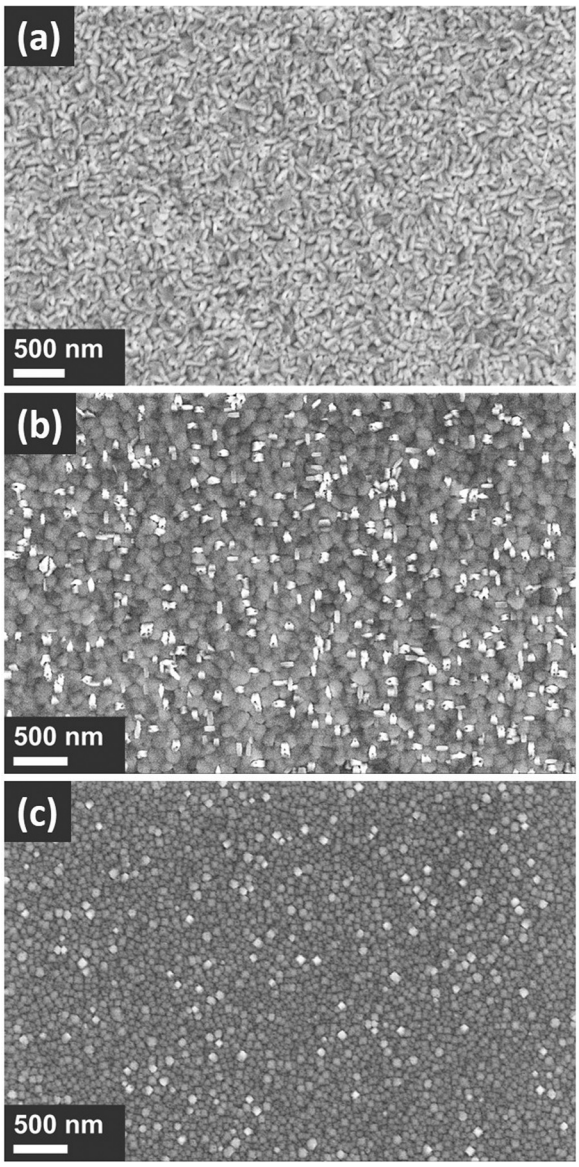

FIG. 2. SEM images of the $NiSi_2$ films in (a) sample *a*, (b) sample *b*, and (c) sample *c*. Sample *a* is $NiSi_2$ grown on the IBAD MgO template using Ar, sample *b* is $NiSi_2$ grown on the IBAD TiN template using Ar, and sample *c* is $NiSi_2$ grown on the IBAD TiN template using Ar mixed with H_2.

As illustrated in Figs. 4(a) and 4(b), $NiSi_2$ has a fluorite structure with a lattice constant of ~0.538 nm, and TiN has a rock-salt structure with a lattice constant of ~0.424 nm. Besides, Si has a diamond structure with a lattice constant of ~0.543 nm, and MgO has the same crystal structure and a close lattice constant as TiN. Due to the low lattice mismatch (0.9%) between Si and $NiSi_2$, the epitaxial growth of Si on $NiSi_2$ is expected. However, the lattice misfit of $NiSi_2$ to TiN is calculated to be around 10.3% from Fig. 3(c), making it intriguing how epitaxial growth of $NiSi_2$ is achieved on TiN but not on MgO.

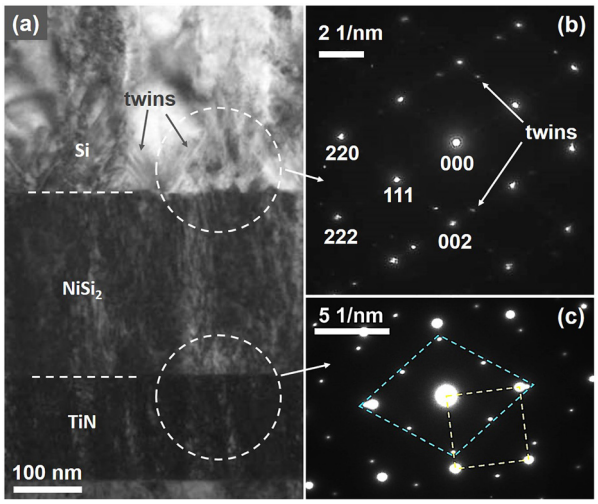

FIG. 3. (a) Bright field cross-sectional TEM image of sample *c* with a Si film grown on $NiSi_2$ (the zone axis is $NiSi_2$ [2$\bar{2}$0]), (b) SAED pattern at the Si-$NiSi_2$ interface, and (c) SAED pattern at the $NiSi_2$-TiN interface. The reciprocal lattices of $NiSi_2$ and TiN are marked with blue dashed lines and yellow dashed lines, respectively. Sample *c* is $NiSi_2$ grown on the IBAD TiN substrate using Ar mixed with H_2.

According to the theory of epitaxial nucleation and growth,[24] the nature of the chemical bonding is another crucial factor affecting the chemical potentials during epitaxial growth. Both $NiSi_2$[25] and TiN[26] have a complex bonding nature, which is composed of localized metal-nonmetal covalent bonds and metal-metal metallic bonds. With an in-plane rotation of 45°, a possible atomic configuration at the interface is depicted in Fig. 4(c). The contact plane is supposed to be the (001) planes of both materials. The bonding similarity makes it possible to form Ni-N and Si-Ti covalent bonds and Ni-Ti metallic bonds, which can in turn significantly reduce the interface energy and promote epitaxial nucleation. In contrast, with ionic bonds formed within the IBAD MgO template in sample *a*, $NiSi_2$ shows non-epitaxial nucleation and growth. A first principles calculation of the $NiSi_2$-TiN interface is underway to confirm the hypothesis.

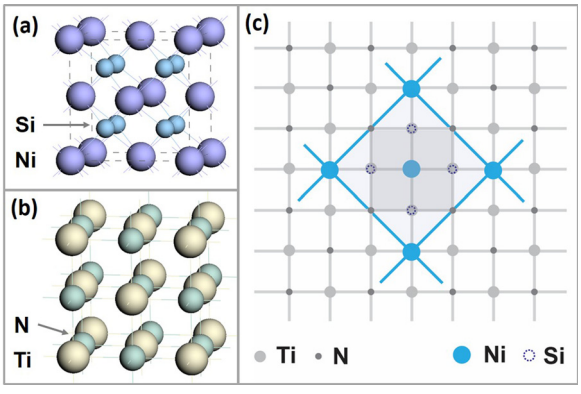

FIG. 4. Ball and stick atomic models of (a) $NiSi_2$ and (b) TiN. (c) An illustrative drawing of the most likely atomic configuration at the $NiSi_2$/TiN interface.

In addition to the interface energy between the film and the substrate, the surface energy of the film also influences the orientation of $NiSi_2$ during nucleation. In polycrystalline sample *a*, the preferred orientations are $NiSi_2$ (111) and $NiSi_2$ (220) instead of $NiSi_2$ (004), which probably results from the relatively high surface energy of $NiSi_2$ (004).[27] Then, in sample *b*, the preferred orientation becomes $NiSi_2$ (004) due to the correspondingly lowered interface energy. However, the low surface energy $NiSi_2$ (220) orientation still exists probably in a metastable phase during the non-equilibrium PVD deposition process. Eventually in sample *c*, the use of the Ar-H_2 mixture eliminates the $NiSi_2$ (220) orientation. Hydrogen atoms are reported to be able to passivate the surface of Si,[28,29] and hence, a similar effect of surface passivation likely happens to $NiSi_2$. Consequently, the surface energy difference between $NiSi_2$ (220) and $NiSi_2$ (004) is mitigated.

Rather than annealing separate Ni and Si phases to form nickel silicides with phase and structural complexity, direct epitaxial growth of a single-phase $NiSi_2$ thin film by sputter deposition of $NiSi_2$ is achieved on low-cost and flexible metal tapes, which is demonstrated by HRXRD, SEM, and TEM measurements. Epitaxial growth of $NiSi_2$ is achieved on homo-epitaxial TiN which is grown on IBAD TiN on metal tapes. The TiN layers serve as the seeding layer and the diffusion barrier. The epitaxial relationship between $NiSi_2$ and TiN is observed as $(001)\langle 100\rangle NiSi_2 \parallel (001)\langle 110\rangle TiN$. In spite of the extra-large lattice mismatch (~10.3%), epitaxial growth of $NiSi_2$ on TiN takes place likely because of the bonding similarity between $NiSi_2$ and TiN. H_2 used during the sputter deposition process helps to passivate the $NiSi_2$ surface and thus eliminate the metastable $NiSi_2$ (220) orientation. The resulting $NiSi_2$ thin film is flat and smooth, composed of grains with a size of 50–100 nm, and free from twins though with large lattice mismatch to the substrate. Epitaxial growth of a Si film is further demonstrated on top of the $NiSi_2$ thin film evident from single-crystalline SAED patterns. The directly sputter-deposited epitaxial $NiSi_2$ thin film over metal substrates offers a promising route to fabricate low-cost, flexible electronic devices with $NiSi_2$/TiN/Hastelloy as the direct contact.

See supplementary material for 3 parts. Part 1 describes the growth parameters of the Si film on sample *c*. Part 2 shows the metal-scale resistivities of the TiN and $NiSi_2$ thin films. Part 3 presents the XRD and SEM data of the Si film on sample *c*.

This study was supported by funding from the U. S. Department of Energy (DOE) SunShot Initiative program (Award #: DEEE0006711).

REFERENCES

[1]N. Breil, C. Lavoie, A. Ozcan, F. Baumann, N. Klymko, K. Nummy, B. Sun, J. Jordan-Sweet, J. Yu, F. Zhu, S. Narasimha, and M. Chudzik, Microelectron. Eng. **137**, 79–87 (2015).
[2]S. Abhaya, G. Amarendra, B. Panigrahi, and K. Nair, J. Appl. Phys. **99**(3), 033512 (2006).
[3]C. L. Hsin and S. S. Deng, Nanotechnology **27**(6), 065704 (2016).
[4]J. Fouet, M. Texier, M. I. Richard, A. Portavoce, D. Mangelinck, C. Guichet, N. Boudet, and O. Thomas, Mater. Lett. **116**, 139–142 (2014).
[5]C. J. Choi, S. Y. Chang, Y. W. Ok, T. Y. Seong, H. Gan, G. Z. Pan, and K. N. Tu, J. Electron. Mater. **32**(10), 1072–1078 (2003).
[6]V. Teodorescu, L. Nistor, H. Bender, A. Steegen, A. Lauwers, K. Maex, and J. Van Landuyt, J. Appl. Phys. **90**(1), 167–174 (2001).
[7]M. Tinani, A. Mueller, Y. Gao, E. A. Irene, Y. Z. Hu, and S. P. Tay, J. Vac. Sci. Technol., B **19**(2), 376–383 (2001).
[8]L. H. Wu and C. J. Tsai, Electrochem. Solid State Lett. **12**(3), H73–H76 (2009).
[9]Y. Gao, Y. Li, and V. Selvamanickam, "Fast ion-beam-assisted-deposition of highly oriented titanium nitride buffer layers directly on low-cost Hastelloy substrates by a roll-to-roll process" (unpublished).
[10]R. Hühne, S. Fähler, and B. Holzapfel, Appl. Phys. Lett. **85**(14), 2744–2746 (2004).
[11]Y. Sun and J. A. Rogers, Adv. Mater. **19**(15), 1897–1916 (2007).
[12]O. Song, Y. Choi, J. Han, and G. Kim, Korean J. Met. Mater. **49**(4), 321–328 (2011).
[13]V. Selvamanickam, S. Sambandam, A. Sundaram, S. Lee, A. Rar, X. Xiong, A. Alemu, C. Boney, and A. Freundlich, J. Crystal Growth **311**(21), 4553–4557 (2009).
[14]Y. K. Li, H. C. Guo, Y. Yao, P. Dutta, M. Rathi, N. Zheng, Y. Gao, S. C. Sun, J. H. Ryou, P. Ahrenkiel, and V. Selvamanickam, CrystEngComm **20**(41), 6573–6579 (2018).
[15]P. Dutta, Y. Gao, M. Rathi, Y. Yao, Y. Li, M. Iliev, J. Martinez, and V. Selvamanickam, Acta Mater. **147**, 51–58 (2018).
[16]M. Rathi, P. Dutta, N. Zheng, Y. Yao, D. Khatiwada, A. Khadimallah, Y. Gao, S. Sun, Y. Li, S. Pouladi, P. Ahrenkiel, J. H. Ryou, and V. Selvamanickam, J. Mater. Chem. C **5**(31), 7919–7926 (2017).
[17]Y. Gao, M. Asadirad, Y. Yao, P. Dutta, E. Galstyan, S. Shervin, K.-H. Lee, S. Pouladi, S. Sun, and Y. Li, ACS Appl. Mater. Interfaces **8**(43), 29565–29572 (2016).
[18]S. Pouladi, M. Rathi, D. Khatiwada, M. Asadirad, S. K. Oh, P. Dutta, Y. Yao, Y. Gao, S. Sun, Y. Li, S. Shervin, K.-H. Lee, V. Selvamanickam, and J.-H. Ryou, Prog. Photovoltaics: Res. Appl. **27**(1), 30–36 (2019).
[19]W. B. Nowak, R. Keukelaar, W. Wang, and A. R. Nyaiesh, J. Vac. Sci. Technol., A **3**(6), 2242–2245 (1985).
[20]M. Finetti, I. Suni, and M. A. Nicolet, J. Electron. Mater. **13**(2), 327–340 (1984).
[21]S.-J. Jeong, D.-I. Kim, S. O. Kim, T. H. Han, J.-D. Kwon, J.-S. Park, and S.-H. Kwon, J. Nanosci. Nanotechnol. **11**(1), 671–674 (2011).
[22]S. H. Kim, K. T. Nam, A. Datta, and K. B. Kim, J. Appl. Phys. **92**(9), 5512–5519 (2002).
[23]P. N. Arendt and S. R. Foltyn, MRS Bull. **29**(8), 543–550 (2004).
[24]I. V. Markov, *Crystal Growth for Beginners: Fundamentals of Nucleation, Crystal Growth, and Epitaxy* (World Scientific, 2003), pp. 357–359.
[25]M. K. Niranjan, V. S. Kumar, and R. Karthikeyan, J. Phys. D: Appl. Phys. **47**(28), 285101 (2014).
[26]N. Savvides and B. Window, J. Appl. Phys. **64**(1), 225–234 (1988).
[27]S. Yamauchi, M. Hirai, M. Kusaka, M. Iwami, H. Nakamura, Y. Yokota, and H. Watabe, Appl. Surf. Sci. **70**(1), 461–465 (1993).
[28]D. Eaglesham, F. Unterwald, and D. Jacobson, Phys. Rev. Lett. **70**(7), 966 (1993).
[29]G. Trucks, K. Raghavachari, G. Higashi, and Y. Chabal, Phys. Rev. Lett. **65**(4), 504 (1990).